UNIVERSITY OF DUNDEE

University of Dundee

Time-resolved single photon spectroscopy through a single optical fibre for miniaturised medical probe design

Ehrlich, K.; Fleming, H.; McAughtrie, S.; Kufcsák, A.; Krstajic, N.; Campbell, C. J.; Henderson, R. K.; Dhaliwal, K.; Thomson, R. R.; Tanner, M. G.

Time-resolved single photon spectroscopy through a single optical fibre for miniaturised medical probe design

K. Ehrlich[*a,b], H. Fleming[d], S. McAughtrie[b,d], A. Kufcsák[c], N. Krstajic[b,c], C. J. Campbell[d], R. K. Henderson[c], K. Dhaliwal[b], R. R. Thomson[a,b], M. G. Tanner[a,b]

[a]Scottish Universities Physics Alliance (SUPA), Institute of Photonics and Quantum Science, Heriot-Watt University, Edinburgh EH144AS, UK,
[b]EPSRC IRC Hub in Optical Molecular Sensing & Imaging, MRC Centre for Inflammation Research, Queen's Medical Research Institute, University of Edinburgh, 47 Little France Crescent, Edinburgh EH164TJ, UK,
[c]Institute for Integrated Micro and Nano Systems, School of Engineering, University of Edinburgh, King's Buildings, Alexander Crum Brown Road, Edinburgh EH93FF, UK,
[d]School of Chemistry, EaStChem, University of Edinburgh, Joseph Black Building, West Mains Road, Edinburgh EH93FF, UK

ABSTRACT

We present a spectroscopic system and an optical fibre probe which enable the full exploitation of the temporal evolution and spectral information of a weak Raman signal against background fluorescence and intrinsic fibre Raman. The system consists of a single multimode fibre and a CMOS single-photon avalanche diode (SPAD) line sensor capable of resolving and histogramming the arrival times of photons for 256 pixels simultaneously, offering improved signal to background compared to a non-time resolved measurement modality. The capabilities of the system are tested for intrinsic Raman standards such as cyclohexane and for pH sensing with functionalised gold nanoshells exploiting surface enhanced Raman scattering (SERS). The nanoshells are functionalised with the pH responsive 4-mercaptobenzoic acid (MBA) enabling demonstration of wide range pH sensing with low excitation power (< 1 mW) and short acquisition times (10 s), achieving a measurement precision of ± 0.07 pH units.

Keywords: Fibre optic sensors, Time-resolved spectroscopy, Photon counting, Raman spectroscopy, Surface-enhanced Raman scattering, Detector arrays

1. INTRODUCTION

In 2012, respiratory diseases were accountable for an average of 20.1 % of all deaths in the UK, with numbers stagnating for the last 10 years while numbers for heart diseases decreased[1]. The total costs in the UK in 2014 were £11.1 bn for treatment and loss to the wider economy[2]. Recent development to tackle this problem include optical imaging through flexible fibre imaging bundles in combination with optical molecular probes based on environmental fluorophores to identify pulmonary infections and inflammation *in vivo*[3,4]. Additionally, the image-guided diagnosis can be supported with localized measurements of key physiological parameters such as pH, oxygen saturation or glucose concentration. We investigate pH as a key marker in this paper, which is tightly regulated in the human body but can locally change due to inflammations and cancerous environments. Furthermore, in the dawn of antimicrobial resistance (AMR), the monitoring and quantification of pH could potentially help clinicians to improve diagnosis and treatment because the growth of bacteria are enhanced in acidic environments while certain antibiotics are inhibited in acidic environments.

Raman spectroscopy investigates the chemical fingerprint of a molecule through its vibrational energy levels by exploiting the inelastic scattering of light when the sample is interacting with light. The advantages are its non-destructiveness, it is minimally invasive, being label-free, and has a rapid response which is important for *in situ* diagnosis[5]. However, the Raman scattering is an inherently weak signal due to the small cross section of the Raman

* Send correspondence to K. Ehrlich: ke9@hw.ac.uk

scattering and the fact that its intensity scales inversely with the excitation wavelength ($1/\lambda^4$-dependency). The *in vivo* Raman signal is further obscured by the background from the optical fibre and the fluorescence of the environment. The optical fibre which is required to gain access to remote hollow areas such as the alveoli region of the lung generates fluorescence and Raman scattering, depending on the excitation wavelength, in its core material. This fibre background, contrary to the fluorescence background from tissue, is constant and scales with the fibre length. The fluorescence from surrounding regions e.g. the autofluorescence of endogenous tissue fluorophores, is heterogeneous within and across samples, and hence very difficult to calibrate out. Efforts in recent years in response to the challenge have included complex set ups and computational methods for fluorescent background suppression[6] and advanced Raman probe designs[7–9]. However, while some are not applicable for *in vivo* applications, others suffer from sophisticated and expensive set-ups or long acquisition times.

To overcome the challenges and enable a background free Raman spectroscopy, we demonstrate a time-correlated single photon counting (TCSPC)[10] spectrometry technique. This approach moves the focus away from advanced and costly endoscopic probe design development because it enables endoscopic spectrometry with a standard single core multimode optical fibre. The fibre is small enough to reach otherwise size restricted regions and simple and cheap enough to be used as a disposable sensing probe. TCSPC capable complementary metal-oxide semiconductor (CMOS) single-photon avalanche diodes (SPAD) line sensors are able to detect single photons and histogram them according to their arrival time for 256 pixels simultaneously which are correlated to different wavelengths[11]. The advantages of these line sensors are high efficiency with a fill-factor of 48 % and high time resolution (< 500 ps time stamping resolution) to record luminescent kinetics down to the nanosecond regime[12,13]. By using the additional information about the temporal evolution we can exploit the different time profiles of background fluorescence, fibre Raman scattering and the Raman from the end of fibre to separate the wanted Raman signal from unwanted background[14–16]. This is done through post-processing time-gating. The technique is currently only limited by photon statistic constraints known as counting loss and pile-up, and inherent limitations on the performance of the SPADs; detector dead-time, dark count rate, varying photon detection probabilities, crosstalk and afterpulsing[10(chap6.2, 7.8, 7.9)]. Others have presented time domain gating techniques such as streak cameras, electronically time-gated CCDs[16] or CMOS detectors[13,17] and optical driven Kerr gates[18]. While the latter achieves a time resolution of picoseconds, the setup is costly and measurement times lengthy – on the order of minutes.

The system is exemplified for pH sensing with 4-mercaptobenzoic acid (MBA) in this paper. Gold nanoshells were functionalised with MBA and then deposited on the distal end of the delivery fibre. These nanosensors have been designed for localized measurements of pH in vivo as they can be used in the near-infrared spectral region, avoiding distortion from excessive autofluorescence from tissue and blood. They are also robust and exhibit a continuous signal over a wide range of pH[19]. The SERS effect enhances the Raman signal and allows low excitation power (< 1 mW) and short exposure times of 10 s with a measurement precision of ± 0.07 pH units is thus achieved. The enhanced signal to background achieved in a time resolved modality is also used to investigate the observation of weak intrinsic Raman signals.

2. MATERIALS AND METHODS

2.1 Experimental Setup

A schematic of the time-resolved spectrometer is shown in Fig. 1.

The whole system is comprised of four parts: a pulsed excitation source, an optical coupling and collection system, a spectrometer and an in-house made CMOS SPAD line sensor. The fibre-coupled design is versatile and flexible for a broad range of applications, a fluorescence spectrometer version of this setup is presented elsewhere[11], and with the potential to be compact and mobile, suitable for *in situ* applications. The excitation source was a 785 nm pulsed laser (LDH-D-F-N-780 and PDL 800-D, PicoQuant, spectral FWHM < 0.35 nm) using the near-infrared window for biological tissue to minimise tissue fluorescence background. In TCSPC methodology the repetition rate of the laser determines the duration of the measurement window. To gather all information within one measurement window, it must be ensured that a full measurement of light transiting the length of the fibre and being backscattered to the detector is completed before the next laser pulse. For a 2.7m fibre used in these experiments, this is achieved with a repetition rate of 20 MHz. The optical coupling and collection system ensures efficient coupling into the delivery fibre and the spectrometer by using a 1:1 imaging system and a fluorescence filter set consisting of an excitation filter, a dichroic
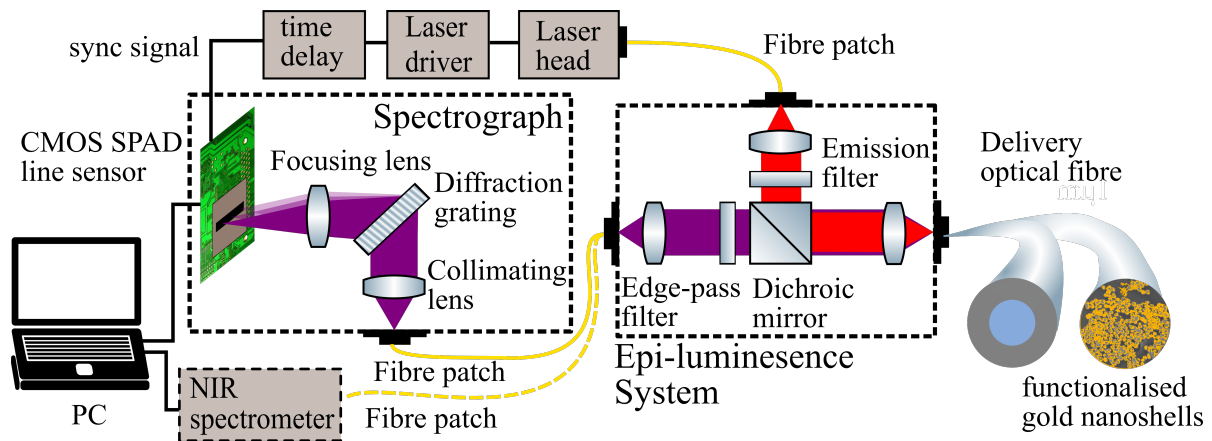
Figure 1: A schematic of the time-resolved spectrometer consisting of a pulsed laser source, an optical coupling and collection system, a transmission spectrograph and a CMOS SPAD line sensor. The delivery optical fibre is a 2.7 m standard step-index single core fibre (FG050LGA, Thorlabs). For the pH sensing, functionalised gold nanoshells are deposit onto the distal end of the fibre.

beam splitter and an emission filter. The spectrometer determines the spectral resolution which is limited by the entrance slit, a multimode fibre with a core diameter of 50 um, the transmission grating (1624 grooves / mm, Wasatch) density the lens combination, a collimation lens (f = 50 mm) and a focusing lens (f = 30 mm, both Achromat Doublets, Thorlabs). The resulting spectral resolution is 1.6 nm or 25 cm^{-1}. A throughput of 78 % at the centre wavelength was measured with a photodiode (S120C Thorlabs). The in-house made CMOS SPAD sensor consists of 256 pixels in a single line manufactured with 130 nm CMOS technology. The whole electronics needed for TCSPC is integrated on a printed circuit board (PCB) exploiting a robust and compact 'system on a chip' design. The sensor timestamps the single photon events internally and simultaneously for all pixels. The average power was reduced with neutral density filters to 0.8 mW which is safe for *in vivo* measurement and ensures single photon regime at a detector count rate of < 1 % of the laser excitation rate and < 50 % of the detector readout frame rate to avoid pile-up distortions. While a high spectral resolution is important to resolve the fine Raman peaks, the temporal resolution determines the capability of separating the Raman signal from the unwanted background signal from the fibre and the environmental fluorescence. The temporal resolution of this system is determined by the time-to-digital converter (TDC) which is 423 ± 3 ps, the full width half maximum (FWHM) of the SPAD which is 0.8 ns and the FWHM of the laser source. When operated at maximum power, the laser has a short leading pulse with a FWHM of 30 ps as stated by the manufacturer, however it exhibits a long tail with a FWHM of 1.5 ns containing ¾ of the power. This greatly limits the temporal resolution and influences the window width in the data analysis.

2.2 Data Analysis

TCSPC is considered a slow method as only one photon per integration time is counted, and as the accuracy of the pH sensing is increasing with the number of counted photons, the number of cycles or measurement time to gather the necessary statistics can be long. In single photon counting (SPC) mode every photon is registered during the integration time, only limited by the dead time of the detector, however the timing information is not available. A combination of TCSPC and SPC is the gating of the signal where a narrow time windows is provided so that the signal of interest, in our case the Raman at the end of the fibre tip, is selected against others. Time-gating can be done either on-chip where the electronics or the SPADs itself are disabled during certain times or during post-processing when the time-resolved data are sliced into certain time windows. In photon starving regimes (approximately 1 photon per laser cycles), which are likely in *in vivo* measurements, there is no advantages of SPC mode over TCSPC mode in terms of measurement time, while TCSPC modality acquires more information.

A single measurement yields a 3-dimensional data cube consisting of the spectral axis, the temporal axis and intensity data in terms of number of counts per pixel and per time bin. For gathering the spectral information, each pixel is correlated to a certain wavelength range. The temporal information is gained by measuring the arrival time of the photons and histogramming them for each pixel with the on-chip TCSPC functionality of the sensor. The full measurement with SERS at the fibre tip can be seen in Figure 2 a). The full measurement is then sectioned into certain time windows depending on the information they contain. The data analysis consists of three steps: i) "Noisy pixels" are

identified and the data removed from the measurement. These pixels are electronically closer to their avalanche condition and hence exhibit a higher dark count (DC) rate. There is a balance to maintain as every pixel for which data is removed worsens the spectral resolution which is critical with the fine Raman peaks. We determine the average DC level from the 'DC' time window, indicated in Figure 2 a), as a threshold and remove pixels which DC rate is 2 times above the average. ii) The 'fibre' window contains solely the information from the backscattered fibre Raman which can be used to determine the spectral shape of the fibre Raman background. This, with a scaling factor, is subtracted from the remaining fibre Raman signal derived from the 'fibre + SERS' time window and thus allows the background free recovering of the MBA Raman spectra. The scaling factor accounts for the forward Raman scattering fibre background reflected on the several surfaces at the fibre tip. Knowing the backscattering fibre Raman spectral shape from every point along the fibre can be used for distributed temperature sensing[20] or checking the integrity of the fibre if not accessible otherwise.

3. RESULTS AND DISCUSSIONS

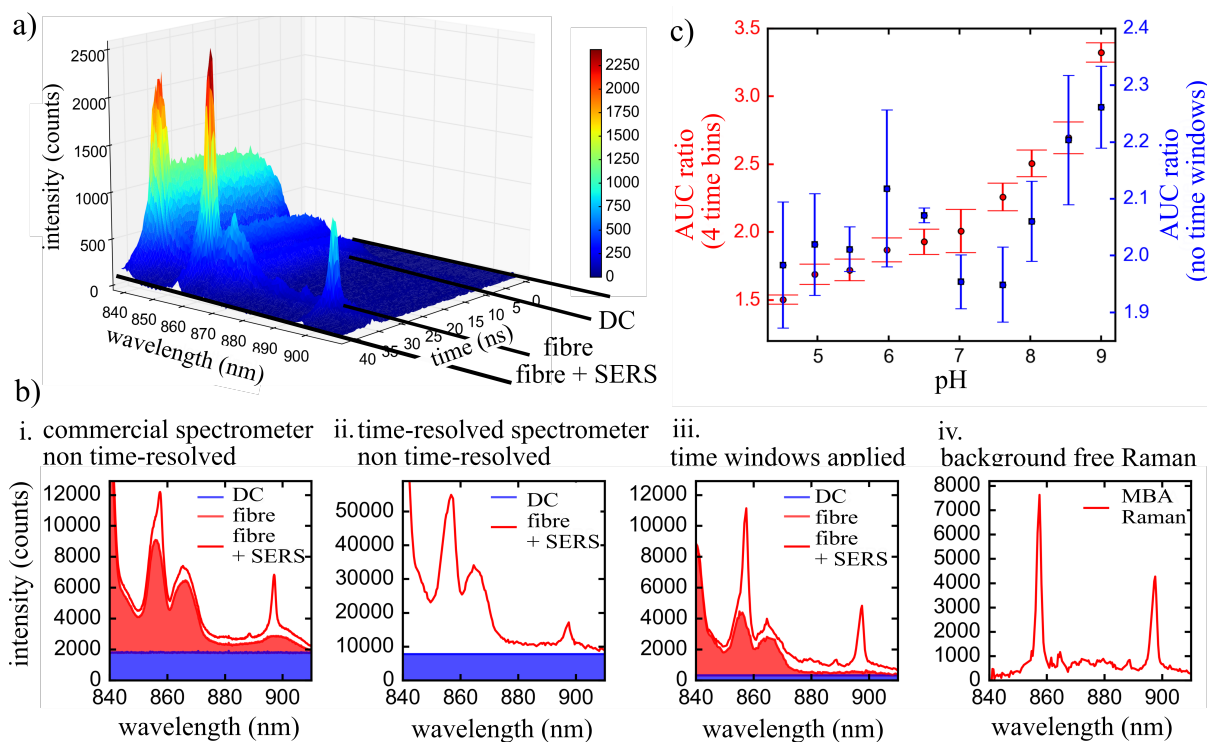### 3.1 Molecular reporter based on surface enhanced Raman scattering (SERS)

Figure 2. a) 3-dimensional representative of a 2.7 m multimode optical fibre with functionalised gold nanoshells at the fibre tip. Noisy pixels are removed and dark counts are subtracted. The time window used in the further analysis are indicated. (b) from left to right: i) Non time-resolved measurement with a commercial spectrometer (QEPro, Ocean Optics). ii) Non time-resolved measurement with the time-resolved spectrometer. iii) Spectra originate when the time windows indicated in (a) are applied. Time window width is 5 time bins or 2.1 ns. iv.) A recovered spectrum from the MBA molecule. Each measurement was obtained using an average excitation power of 0.8 mW and 20 MHz pulse repetition rate and an integration time of 10 s. (c) pH sensing using the variation of area under the curve (AUC) ratio, the error bars represent the standard deviation of the mean over 3 replicate measurements.

Figure 2 b) i. and ii. shows that the time-resolved spectrometer arrives at visually similar spectra when compared to a commercial spectrometer. However, it also offers a higher efficiency but a lower spectral resolution which leads to a broadening and a lower peak visibility for the SERS features at ~860 nm and ~900 nm. At the same time, the ratio of DC to signal is comparable between both spectrometers. Through post-processing time-gating, the detector dark counts and the unwanted fibre Raman can be significantly suppressed and the visibility of the SERS Raman signal can be significantly increased, as shown in Figure 2 b) iii. with a temporal window of 5 time bins or 2.1 ns, the S/B improves by 4× for a dark count dominated background, around the 857 nm peak, and by 19× around the 897 nm peak when

comparing the time-gated results with the measurements from a commercial spectrometer. When applying the time windows to the data, the background photon shot noise is reduced by a factor equal to the square root of the number of which the time bins are reduced from the full time-resolved measurement. The background free MBA Raman spectra (Figure 2 b) iv. can be used for pH sensing by using the area under the curve (AUC) ratio of the two pH sensitive spectral features of MBA around 880 nm and 906 nm. The results shown in Figure 2 c) are for a 10 s measurement time and show that the sensitivity can be greatly increased through applying the time windows. The repeatability of the system was measured through 50 consecutive measurements of pH 6 and pH 8 to be 0.14 and 0.19, respectively. The sensitivity and repeatability can be further increased through a longer integration time. Suppression of environmental fluorescence with this methodology is show elsewhere[21]. The limitations of this analysis are the IRF function of the laser and the temporal stability of the CMOS SPAD line sensor. As mentioned above the time profile of the laser is ~2 ns which was shown to be the best time window width size for our analysis. If the pulse width of the laser and the IRF of the SPADs, which have been shown to be 0.8 ns[13] were shorter then shorter time window width is achievable and favorable in terms of distinguishing Raman and fluorescence background. In terms of accuracy, the limits of the line sensor were reached and improvements have to include further detector calibrations such as photon-detection variations and reduction of the dark counts and shot noise through cooling and active temperature stabilization. The time-gating method in this paper is achieved by recording a whole TCSPC measurement and applying time windows to the data during post-processing. Electronic time-gating introduces additional jitter to the measurement through the enabling and disabling of the detector but potentially decreases the measurement time.

3.2 Intrinsic Raman

The surface-enhancing effect of the gold nanoshells enables strong and easily detectable MBA Raman signal, however, label-free sensing would rely on the intrinsic Raman. The near-infrared window for biological tissue exhibits low tissue Raman, and would be useful for deep tissue Raman which requires higher excitation powers than we can achieve with
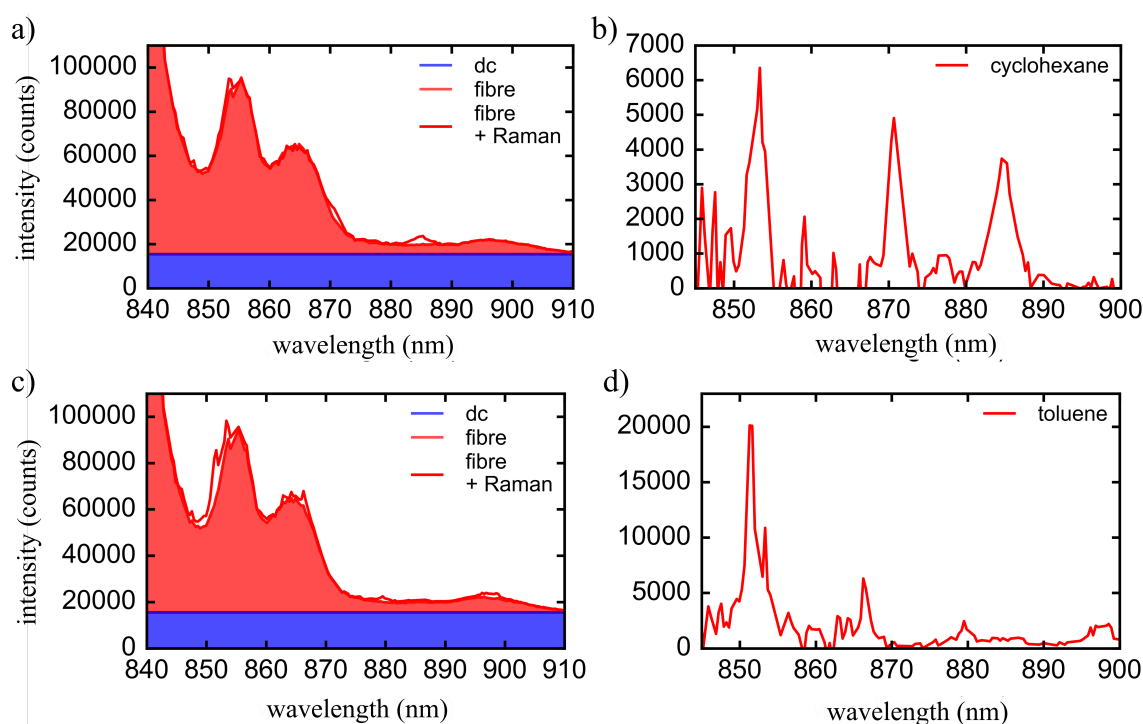

Figure 3. a) Time resolved measurement of Raman scattering from cyclohexane through a 2.7m optical fibre. The time windows are applied as shown in Fig. 2 with a time window width of 6 time bins or 2.5 ns. b) Background free Raman spectra from cyclohexane c) Time resolved measurement of Raman scattering from toluene through a 2.7m optical fibre. The time window width is 6 time bins or 2.5 ns. (d) Background free Raman spectra from toluene. The data analysis followed the same methodology as presented in Figure 2 b). Each measurement was obtained using an average excitation power of 1.2 mW and 20 MHz pulse repetition rate and an integration time of 300 s.

our laser. Instead, we demonstrate the capabilities of our system with standard Raman example chemicals which have a strong intrinsic Raman signal – cyclohexane and toluene. To compensate for the weak signal, the integration time was increased to 300 s, otherwise the experimental conditions are identical to the SERS measurements. A time window width of 6 time bins or 2.5 ns was used which reduces the background count rate and the background noise by a factor of 19.

In Figure 3, the same data analysis method of post-processing time-gating was applied to the raw data and we were able to retrieve the background free Raman spectra of cyclohexane and toluene. In Figure 3 c), the three strong Raman lines of cyclohexane at 854 nm (1027 cm^{-1}), 871 nm (1266 cm^{-1}) and 885 nm (1443 cm^{-1}) are visible in similar peak intensities which is expected from literature[22]. Small variations to the intensities are due to chromatic aberration in the spectrometer's optical system. The smaller peak at 863 nm (1157 cm^{-1}) is hardly visible as it is just above the noise level. In Figure 3 d), the Raman lines of toluene are shown. The two close peaks around 852 nm and 854 nm, 1003 cm^{-1} and 1030 cm^{-1} respectively, are visible as a double peak because the peak separation is the same order as the spectral resolution of the spectrometer and hence not resolvable. The Raman lines of lower intensity at 867 nm (1200 cm^{-1}), 880 nm (1380 cm^{-1}) and 897 nm (1600 cm^{-1}) are visible. We show that we can see the strong peaks of the intrinsic Raman samples. While we are limited by the noise level for observation of the weaker peaks, it is clear there is a great improvement in visibility of intrinsic Raman features through the time resolved methodology As discussed above further improvement in terms of reducing the dark counts, enhancing the temporal stability of the detector and increasing the laser power will help to enhance the sensitivity of the system for intrinsic Raman measurement.

4. CONCLUSION

A time-resolved system and methodology for recovering the spectra of inherently weak Raman signals measured through a single core multimode optical fibre has been demonstrated. We were able to enhance the visibility of the Raman spectra through post-processing time-gating as well as recover them free from background signals such as the fibre Raman and fluorescent environments. As an example, the methodology was applied to standards of intrinsic Raman spectroscopy and to pH-sensing with nanosensors deposited on the distal end of the fibre tip. It has high potential as an ultra-miniaturized and simplified Raman probe for *in vivo* endoscopic sensing of physiological parameters such as pH, oxygen or glucose concentration. While using the SERS effect for the pH nanosensors, measurement times as short as 10 s were used while intrinsic Raman spectra were recorded over a 300 s integration time. Shorter acquisition times are crucial for real-time in situ diagnosis scenarios and the system can be further improved by increasing the collection efficiency through reducing the information the system gathers. Instead of acquiring the full temporal and spectral information, one can bin pixels together and only record the two narrow spectral bands which show the pH sensitive response. However, we believe that time-gating in single photon counting (SPC) modality has no time advantage over TCSPC measurements in low light scenarios such as expected for *in vivo* sensing as measurement rate is limited by photon budget, not detector readout. In applications which are not limited by the photon budget, the on-chip time-gating capabilities of this detector which have been previously demonstrated[13], can be used to further decrease the integration time. To keep the advantage of automatic calibration, multiple time windows would be preferable. The exploitation of this advanced measurement system enables suppression of the unwanted background in the fibre-based Raman probe, facilitating the recovery of the background free spectrum in a single fibre probe.

REFERENCES

[1]   "The battle for breath - the impact of lung disease in the UK.", Br. Lung Found., 26 May 2016, <https://www.blf.org.uk/policy/the-battle-for-breath-2016> (16 April 2018).

[2]   "The battle for breath - the economic burden of lung disease.", Br. Lung Found., 9 March 2017, <https://www.blf.org.uk/policy/economic-burden> (16 April 2018).

[3]   Thiberville, L., Salaün, M., Lachkar, S., Dominique, S., Moreno-Swirc, S., Vever-Bizet, C. and Bourg-Heckly, G., "Human in vivo fluorescence microimaging of the alveolar ducts and sacs during bronchoscopy," Eur. Respir. J. **33**(5), 974–985 (2009).

[4]   Craven, T. H., Walsh, T. S. and Dhaliwal, K., "Emerging Technology Platforms for Optical Molecular Imaging and Sensing at the Alveolar Level in the critically ill," [Annual Update in Intensive Care and Emergency Medicine 2018], Springer, Cham, 247–262 (2018).

[5] Hanlon, E. B., Manoharan, R., Koo, T. W., Shafer, K. E., Motz, J. T., Fitzmaurice, M., Kramer, J. R., Itzkan, I., Dasari, R. R. and Feld, M. S., "Prospects for in vivo Raman spectroscopy," Phys. Med. Biol. **45**(2), R1-59 (2000).

[6] Wei, D., Chen, S. and Liu, Q., "Review of Fluorescence Suppression Techniques in Raman Spectroscopy," Appl. Spectrosc. Rev. **50**(5), 387–406 (2015).

[7] Utzinger, U. and Richards-Kortum, R. R., "Fiber optic probes for biomedical optical spectroscopy," J. Biomed. Opt. **8**(1), 121–147 (2003).

[8] Stevens, O., Petterson, I. E. I., Day, J. C. C. and Stone, N., "Developing fibre optic Raman probes for applications in clinical spectroscopy," Chem. Soc. Rev. **45**(7), 1919–1934 (2016).

[9] Choudhury, D., Tanner, M. G., McAughtrie, S., Yu, F., Mills, B., Choudhary, T. R., Seth, S., Craven, T. H., Stone, J. M., Mati, I. K., Campbell, C. J., Bradley, M., Williams, C. K. I., Dhaliwal, K., Birks, T. A. and Thomson, R. R., "Endoscopic sensing of alveolar pH," Biomed. Opt. Express **8**(1), 243–259 (2017).

[10] Becker, W., [Advanced Time-Correlated Single Photon Counting Techniques], Springer Berlin Heidelberg, Berlin, Heidelberg (2005).

[11] Ehrlich, K., Kufcsák, A., Krstajić, N., Henderson, R. K., Thomson, R. R. and Tanner, M. G., "Fibre optic time-resolved spectroscopy using CMOS-SPAD arrays," Proc. SPIE **10058**, 100580H (2017).

[12] Krstajić, N., Levitt, J., Poland, S., Ameer-Beg, S. and Henderson, R., "256 × 2 SPAD line sensor for time resolved fluorescence spectroscopy," Opt. Express **23**(5), 5653–5669 (2015).

[13] Kufcsák, A., Erdogan, A., Walker, R., Ehrlich, K., Tanner, M., Megia-Fernandez, A., Scholefield, E., Emanuel, P., Dhaliwal, K., Bradley, M., Henderson, R. K. and Krstajić, N., "Time-resolved spectroscopy at 19,000 lines per second using a CMOS SPAD line array enables advanced biophotonics applications," Opt. Express **25**(10), 11103–11123 (2017).

[14] Rojalin, T., Kurki, L., Laaksonen, T., Viitala, T., Kostamovaara, J., Gordon, K. C., Galvis, L., Wachsmann-Hogiu, S., Strachan, C. J. and Yliperttula, M., "Fluorescence-suppressed time-resolved Raman spectroscopy of pharmaceuticals using complementary metal-oxide semiconductor (CMOS) single-photon avalanche diode (SPAD) detector," Anal. Bioanal. Chem. **408**(3), 761–774 (2016).

[15] Kostamovaara, J., Tenhunen, J., Kögler, M., Nissinen, I., Nissinen, J. and Keränen, P., "Fluorescence suppression in Raman spectroscopy using a time-gated CMOS SPAD," Opt. Express **21**(25), 31632–31645 (2013).

[16] Nissinen, I., Nissinen, J., Keränen, P., Länsman, A. K., Holma, J. and Kostamovaara, J., "A Multitime-Gated SPAD Line Detector for Pulsed Raman Spectroscopy," IEEE Sens. J. **15**(3), 1358–1365 (2015).

[17] Erdogan, A. T., Walker, R., Finlayson, N., Krstajic, N., Williams, G. O. S. and Henderson, R. K., "A 16.5 giga events/s 1024 x 8 SPAD line sensor with per-pixel zoomable 50ps-6.4ns/bin histogramming TDC," 2017 Symp. VLSI Circuits, C292–C293 (2017).

[18] Matousek, P., Towrie, M., Ma, C., Kwok, W. M., Phillips, D., Toner, W. T. and Parker, A. W., "Fluorescence suppression in resonance Raman spectroscopy using a high-performance picosecond Kerr gate," J. Raman Spectrosc. **32**(12), 983–988 (2001).

[19] Bishnoi, S. W., Rozell, C. J., Levin, C. S., Gheith, M. K., Johnson, B. R., Johnson, D. H. and Halas, N. J., "All-optical nanoscale pH meter," Nano Lett. **6**(8), 1687–1692 (2006).

[20] Dyer, S. D., Tanner, M. G., Baek, B., Hadfield, R. H. and Nam, S. W., "Analysis of a distributed fiber-optic temperature sensor using single-photon detectors," Opt. Express **20**(4), 3456 (2012).

[21] Ehrlich, K., Kufcsák, A., McAughtrie, S., Fleming, H., Krstajic, N., Campbell, C. J., Henderson, R. K., Dhaliwal, K., Thomson, R. R. and Tanner, M. G., "pH sensing through a single optical fibre using SERS and CMOS SPAD line arrays," Opt. Express **25**(25), 30976–30986 (2017).

[22] "NIST Chemistry WebBook.", <https://webbook.nist.gov/chemistry/> (17 April 2018).